Published in final edited form as:
Exp Neurol. 2010 August ; 224(2): 438–447. doi:10.1016/j.expneurol.2010.05.004.

Lrrk2 Localization in the Primate Basal ganglia and Thalamus: A Light and Electron Microscopic Analysis in Monkeys

H. Lee[1], **H.L. Melrose**[3], **M. Yu**[3], **Jean-Francois Pare**[1], **M.J. Farrer**[3], and **Y. Smith**[1,2]

[1]Yerkes National Primate Research Center, Emory University, Atlanta, GA 30322

[2]Department of Neurology, Emory University, Atlanta, GA 30322

[3]Molecular Genetics Laboratory and Core, Morris K. Udall Parkinson's Disease Research Center of Excellence, Mayo Clinic, Dept Neuroscience, Jacksonville, FL 32224, USA

Abstract

The Leucine Rich Repeat Kinase-2 (*LRRK2*) gene is a common mutation target in Parkinson's disease (PD), but the cellular mechanisms by which such mutations underlie the pathophysiology of PD remain poorly understood. Thus, to better characterize the neuronal target sites of *LRRK2* mutations in the primate brain, we studied the cellular and ultrastructural localization of Lrrk2 immunoreactivity in the monkey basal ganglia. As previously described, the monkey striatum was the most enriched basal ganglia structure in Lrrk2 labeling. Both projection neurons and parvalbumin-containing GABAergic interneurons displayed Lrrk2 immunoreactivity. At the electron microscopic level, striatal Lrrk2 labeling was associated predominantly with dendritic shafts and subsets of putative glutamatergic axon terminals. At the pallidal level, moderate cellular Lrrk2 immunostaining was found in the external globus pallidus (GPe), while neurons in the internal globus pallidus (GPi) were devoid of Lrrk2 immunoreactivity. Strong labeling was associated with cholinergic neurons in the nucleus basalis of Meynert. Midbrain dopaminergic neurons in the primate substantia nigra pars compacta (SNc) and ventral tegmental area harbored a significant level of Lrrk2 labeling, while neurons in the subthalamic nucleus were lightly immunostained. Most thalamic nuclei were enriched in Lrrk2 immunoreactivity, except for the centromedian nucleus that was completely devoid of labeling. Thus, Lrrk2 protein is widely distributed in the monkey basal ganglia, suggesting that gene mutations in PD may result in multifarious pathophysiological effects that could impact various target sites in the functional circuitry of the primate basal ganglia.

Keywords

striatum; putamen; caudate nucleus; Parkinson's disease; substantia nigra; subthalamic nucleus; centromedian nucleus; globus pallidus; dopamine

Correspondence: Yoland Smith, PhD, Yerkes National Primate Research Center, Emory University, 954, Gatewood Rd NE, Atlanta, GA 30322, USA, Tel: (404) 727 7519, Fax: (404) 727 3278, ysmit01@emory.edu.

Introduction

Mutations in Leucine Rich Repeat Kinase-2 (*LRRK2*) gene are the most common cause of late-onset autosomal dominant Parkinson's disease (PD) (Mata et al., 2006; Taylor et al., 2006; Melrose, 2008; Gasser, 2009). Many mutations of the *LRRK2* gene have been identified which can account for as much as 40% of autosomal dominant PD depending on the ethnicity and geographical populations of patients studied (Lesage et al., 2005, 2007; Taylor et al., 2006; Mata et al., 2006; Gandhi et al., 2009). The *LRRK2* gene encodes for a large protein of which the *in vivo* function remains ambiguous. Increased kinase activity likely contributes to some aspects of the disease in patients with the most common *LRRK2* mutation, the G2019S, but other mutations including those in the GTPase domain may also affect kinase activity (Smith et al., 2006; West et al., 2007; Jaleel et al., 2007; Melrose, 2008; Anand and Braithwaite, 2009; Gandhi et al., 2009; Liou and Gallo, 2009). There is evidence that *LRRK2* mutation in PD could result in the dysregulation of vesicular trafficking and transport (Biskup et al., 2006; Greggio et al., 2006; Gandhi et al., 2008; Shin et al., 2008) and alterations in neurites outgrowth (Gillardon, 2009; Parisiadou et al., 2009).

In an effort to decipher the function of Lrrk2 protein in the brain, maps of *LRRK2* mRNA and protein expression have been published in rodents (Biskup et al., 2006; Galter et al., 2006; Melrose et al., 2006, 2007; Simon-Sanchez et al., 2006; Taymans et al., 2006; Higashi et al., 2007b; Westerlund et al., 2008). A common finding of these studies is that *LRRK2* mRNA and protein are most heavily expressed within dopaminoceptive regions of the mammalian CNS, like the striatum and the olfactory tubercle. Surprisingly, a relatively low level of *LRRK2* mRNA expression was observed in dopaminergic neurons of the substantia nigra (Galter et al., 2006; Melrose et al., 2006; Simon-Sanchez et al., 2006). However, recent immunohistochemical studies reported Lrrk2 protein expression in the cortex, striatum, olfactory tubercle, nucleus accumbens, thalamus, hippocampus, septal nuclei, cerebellum and substantia nigra in rats and mice (Biskup et al., 2006; Higashi et al., 2007b; Greggio et al., 2006; Melrose et al., 2007). Overall, the regional distribution of Lrrk2 immunoreactivity in rodents is similar to that recently described in qualitative human brain studies, though some discrepancies have been raised regarding the expression of Lrrk2 in Lewy bodies or Lewy neurites, the pathological hallmark of Parkinson's disease (Giasson et al., 2006; Greggio et al., 2006; Miklossy et al., 2006; Zhu et al., 2006a, 2006b; Higashi et al., 2007a, [2009]; Melrose et al., 2007; Covy et al., 2009; Qing et al., 2009; Waxman et al., 2009).

In order to further characterize the cellular localization of Lrrk2 in the primate brain, we undertook a detailed analysis of Lrrk2 protein expression in the basal ganglia and related thalamic nuclei of rhesus monkeys. To get further insights into the potential intracellular role of Lrrk2 in striatal neurons, this study was complemented with a detailed electron microscopic analysis of Lrrk2 immunoreactivity in the caudate nucleus and putamen.

Materials and Methods

Animals

A total of four adult Rhesus monkeys (*Macaca mulatta*; Yerkes National Primate Research Center colony) were used in this study. The animals used for electron microscopic analysis were 9 to 12 years old at the time of perfusion. One three-year-old monkey was used for light microscopic analysis only. All animal use was in accordance with National Institutes of Health guidelines and was approved by the Emory University Institutional Animal Care and Use Committee. Adequate measures were taken to minimize pain or discomfort. After deep anesthesia with an overdose of pentobarbital (30 mg/kg, i.v.), the monkeys were perfusion-fixed with a cold oxygenated Ringer's solution and a fixative containing 3.75% acrolein and

2% paraformaldehyde in phosphate buffer (PB; 0.1 M, pH 7.4). The brains were then removed from the skull, postfixed for 12 hours in 2% paraformaldehyde and sliced into 60μm-thick coronal sections with a vibrating microtome.

Primary antibodies

An affinity-purified rabbit polyclonal antiserum (PA0362) raised against a synthetic peptide made to the C-terminal region, within residues 2507–2527 of the human Lrrk2 protein was used in the present study.The specificity of this antibody, which is now commercially available from Novus Biologicals (NB110-8771SS; Littleton, CO, USA), has been carefully tested in previous studies, and found to recognize a specific band at a molecular weight that corresponds to that of Lrrk2 protein in immunoblots of rat brain tissue (Melrose et al., 2007). Because of the high inter-species sequence homology of the epitope chosen to generate these antibodies, they were found to react positively against primate and nonprimate brain tissue (Melrose et al., 2007; Novus Biologicals datasheet). Because LRRK2 knockout animals were not available at the time Melrose et al (2007) published data on the specificity of this antibody, we complemented their data with additional immunoblot experiments using brain tissue from LRRK2 knock out mice recently developed in Dr Farrer laboratory (Melrose et al., unpublished data). These knockout animals were created via gene targeting techniques to ablate murine *LRRK2* exon 41. The immunoblot experiments were performed as follows: Sixty micrograms of brain lysate was electrophoresed on a 3–8% Tris-acetate gel and immunoblotted with the polyclonal Lrrk2 antiserum PA062 diluted at 1:500. For the analysis of Lrrk2 protein, 5 volumes of homogenization buffer [50 mM $NaB_{2B}POB_{4,\ B}$10 mM $NaB_{4B}PB_{2B}OB_{7B}$.10$HB_{2B}O$, 20 mM NaF, 2 mM EGTA, 2 mM EDTA, 2 mM $NaB_{3B}VOB_{4B}$,$B_{\ B}$2 mM DTT, protease inhibitor cocktail (Sigma, St. Louis, MO) and phosphatase inhibitor cocktails I and II (Sigma)] were added to one volume of freshly dissected brain tissue. Samples were then homogenized and centrifuged at 12,000x*g* for 5 minutes at 4°C. The supernatant corresponding to the cytosolic fraction was collected and the concentration determined using BCA protein assay reagents (Pierce Biotechnology, Inc/ThermoFisher Scientific Rockford, IL). Samples were denatured in sodium dodecyl sulphate sample buffer before being resolved on a 3–8% Tris-acetate gel (Invitrogen). Blots were blocked in 5% non-fat milk in Tris buffered-saline-Tween and probed with primary antibody overnight at 4°C (PA0362 1:500, Novus # NB110-58771). After incubation with anti-rabbit conjugated secondary antibody (Jackson Immunoresearch Labs, West Grove, PA) bands were visualized using enhanced chemiluminescence (Pierce Biotechnology). Glyceraldehyde 3-phosphate dehydrogenase (GAPDH) was used as a loading control. As shown in figure 1, the antibody was found to detect human Lrrk2 in hWT TG (BAC mice expressing human wild type Lrrk2) and murine Lrrk2 in NT (non-transgenic control), but the Lrrk2 band was absent when the antibody was applied on LKO (*LRRK2* Knockout mouse) brain tissue.

For the immunofluorescent co-localization studies, mouse monoclonal anti-parvalbumin, (PV 235; Swant, Bellinzona, Switzerland) and mouse monoclonal anti-calretinin (CR 6B3; Swant, Bellinzona, Switzerland) antibodies were used. These two antibodies have been extensively used and found to be highly specific for their corresponding antigens in mammalian brain (Celio et al., 1988; Zimmermann and Schwaller, 2002).

Immunoperoxidase labeling for light microscopy (LM)

Sections processed for light microscopy were pre-incubated in phosphate buffered saline (PBS; 0.01M, pH 7.4) containing 1% normal goat serum (NGS), 1% bovine serum albumin (BSA), and 0.3% Triton X-100 for one hour at room temperature (RT), followed by the primary antibody solution containing LRRK2 antibody raised in rabbit (PB0362, in house diluted 1:250), 1% NGS, 1% BSA, and 0.3% Triton X-100 in PBS for 24 hours at RT. After

rinsing in PBS, the sections were incubated in secondary biotinylated goat anti-rabbit IgG (Vector Laboratories, Burlingame, CA; diluted 1:200) for 90 minutes. After washing, sections were incubated for another 90 minutes with the avidin-biotin peroxidase complex (ABC) at a dilution of 1:100 (Vector Laboratories). Finally, sections were washed in PBS and Tris buffer (50 mM; pH 7.6) and transferred to a solution containing 0.025% 3, 3′-diaminobenzidine tetrahydrochloride (DAB; Sigma), 10 mM imidazole, and 0.005% hydrogen peroxide in Tris buffer for 10 minutes. Sections were rinsed in PBS, mounted onto gelatin-coated slides, dehydrated, and then coverslipped with Permount. The basal ganglia nuclei at different levels were examined with a Leica DMRB microscope (Leica Microsystems, Inc., Bannockburn, IL) and images were taken with a CCD camera (Leica DC 500) controlled by Leica IM50 software.

Immunoperoxidase labeling for electron microscopy (EM)

After sodium borohydride treatment, sections were placed in a cryoprotectant solution for 20 minutes (PB 0.05M, pH 7.4, 25% sucrose, and 10% glycerol), frozen at −80°C for 20 minutes, returned to a decreasing gradient of cryoprotectant solutions, and rinsed in PBS. Sections were then incubated in primary and secondary antibody solutions identical to those used for light microscopy; with two exceptions: 1) omission of Triton X-100 and 2) incubation in primary antibody for 48 hours at 4°C.

After DAB reaction, the sections were rinsed in PB (0.1 M, pH 7.4) and postfixed with 1% OsO_4 for 20 minutes. They were then returned to PB and dehydrated with increasing concentrations of ethanol. With the exposure to 70% ETOH, 1% uranyl acetate was added to the solution for 35 minutes to increase the contrast of the tissue at the electron microscope. After dehydration in increasing concentrations of alcohol, sections were further dehydrated with propylene oxide and embedded in epoxy resin for 12 hours (Durcupan ACM; Fluka, Buchs, Switzerland), mounted onto slides, and placed in a 60°C oven for 48 hours. Two blocks of tissues were collected from the caudate nucleus and putamen at both pre and post commissural levels. Blocks of tissue were mounted onto resin blocks, and cut into 60-nm-thick ultrathin sections with an ultramicrotome (Leica Ultracut T2). These sections were collected on Pioloform-coated copper grids, stained with lead citrate for 5 minutes to enhance tissue contrast, and examined on the Zeiss EM-10C electron microscope (Smith and Bolam, 1992).

For each monkey, about 400 electron micrographs of labeled elements were randomly photographed at 25,000X magnification with a CCD camera (DualView 300W; Gatan, Inc., Pleasanton, CA) controlled by Digital Micrograph software (version 3.10.1; Gatan, Inc.). Each micrograph represented an area of approximately 12.56 μm^2. To make sure that Lrrk2 antibodies had full access to antigenic sites, the electron microscopic analysis was performed on the material collected exclusively from the most superficial sections of the blocks. Some of the digitally acquired electron micrographs were adjusted only for brightness or contrast in either the Digital Micrograph software or Adobe Photoshop 8.0. Micrographs were then compiled into figures in Adobe Illustrator 11.0. Statistics were carried using the SigmaStat 2.03 software. All data were expressed as means ± S.E.M and were compared by t-test to determine statistical differences.

Confocal Immunofluorescence Co-localization Studies

Series of five putamen sections from three monkeys were used for the immunofluorescence co-localization studies of Lrrk2 in parvalbumin- and calretinin-immunoreactive striatal interneurons. These sections were first processed with 1% sodium borohydride for 20 min., thoroughly washed in PBS and pre-incubated for 1 hr at room temperature in a solution containing 1% NGS, 1% BSA and 0.3% Triton-X-100 before being incubated overnight at

room temperature in primary antibody solutions (Rabbit anti-Lrrk2-1:400/Mouse anti-CR-1:5000 or Rabbit anti-Lrrk2-1:400/Mouse anti-PV-1:1000). Following PBS washes, sections were incubated for 2 hours at room temperature in a cocktail of secondary antibodies [1:200 biotinylated goat anti-rabbit IgGs, (Vector Labs, Burlingame, CA, USA) + 1:100 FITC-Donkey anti-mouse IgGs, (Jackson Immunoreasearch, West Grove, PA, USA)] in the same diluting solutions as used for primary antibodies. This was followed by 2 hours incubation in a TRITC-coupled streptavidin solution and rinses before being mounted on gelatin-coated slides and coverslipped with Vectashield (Vector Labs, Burlingame, CA, USA). The material was analyzed in a Zeiss LSM 400 confocal microscope. A total of 200 PV- and CR-positive neurons were randomly selected and tested for co-localization with Lrrk2 immunoreactivity from the 15 striatal sections processed in each animal.

Results

Lrrk2 Protein Immunoreactivity in Monkey Basal Ganglia

At the light microscopic level, Lrrk2 immunoreactivity was strongly expressed throughout the monkey brain, but structures such as the striatum, the cerebral cortex, the substantia nigra and the thalamus were most particularly enriched in cellular and neuropil Lrrk2 labeling. Although all basal ganglia nuclei contained a significant level of Lrrk2 immunostaining, the caudate nucleus, putamen and nucleus accumbens were, by far, the most strongly labeled brain regions. The striatal distribution of labeling was quite homogeneous throughout its entire extent without any evidence for structural or regional differences in labeling intensity between functional striatal territories or between the patch (or striosomes) and matrix compartments (Fig. 2). At the cellular level, the Lrrk2 immunoreactivity was expressed in numerous lightly labeled small- to medium-sized perikarya (Fig. 3A) and a subset of large neuronal cell bodies, which likely corresponded to interneurons (Fig. 3A). In addition, fine distal processes formed a dense matrix of diffuse Lrrk2 immunoreactivity which could only be further characterized at the electron microscopic level (see below).

In order to further characterize the chemical phenotype of these interneurons, we performed an immunofluorescent co-localization study with two markers of the main populations of GABAergic interneurons in the primate striatum. This analysis revealed that 97% of parvalbumin-positive interneurons displayed Lrrk2 immunoreactivity (N=200), while only 3% of calretinin-containing neurons were Lrrk2-positive (N=200) (Fig. 4). There was no difference in the degree of co-localization between the caudate nucleus and putamen.

In contrast to the striatum, Lrrk2 immunoreactivity in the globus pallidus was mainly localized in neuronal perikarya that lay within a lightly labeled neuropil. Despite the relatively light labeling compared with the striatum, a significant difference in the degree of cellular labeling was noticed between the internal (GPi) and external (GPe) pallidal segments, ie the GPe harbored a much larger number of immunoreactive neuronal cell bodies than GPi (Fig. 3C, D). In both GPe and GPi, we observed immunoreactive fiber-like processes that likely corresponded to dendritic and axonal segments throughout the nuclei. In addition to pallidal neurons, a population of large neuronal cell bodies along the medullary lamina, that presumably correspond to the cholinergic cell groups of the nucleus basalis of Meynert, displayed strong Lrrk2 immunoreactivity (Fig. 3B,D).

The cell bodies and dendrites of dopaminergic neurons in the dorsal and ventral tiers of the SNc (SNc-d and SNc-v) and ventral tegmental area (VTA) displayed strong Lrrk2 immunoreactivity (Fig. 5B, C, and D). The SN/VTA complex stood out in the ventral midbrain by its dense diffuse neuropil immunostaining that extended into the SN pars reticulata (Fig. 5A). Although no obvious regional pattern of Lrrk2 immunoreactivity could

be disclosed, the medial part of the SN close to the VTA displayed the strongest level of neuropil immunostaining at all rostrocaudal levels (Fig. 5A).

In the subthalamic nucleus, the Lrrk2 immunoreactivity was largely confined to neuronal perikarya with very light neuropil immunostaining. The moderately labeled cell bodies were distributed throughout the whole extent of the nucleus without any obvious pattern of regional distribution (Fig. 5A, E).

Lrrk2 Immunoreactivity in the Monkey Thalamus

Overall, all thalamic nuclei, except the centromedian nucleus (CM), were enriched in Lrrk2 immunoreactivity (Fig. 6). The labeling was particularly strong in neuronal cell bodies, proximal dendrites and neuropil processes. There was a striking difference in the level of immunostaining between the CM and other thalamic nuclei, including the parafascicular nucleus (Pf) (Fig. 6A). Although most thalamic structures were enriched in darkly stained neuronal cell bodies, the CM was almost completely devoid of Lrrk2 immunoreactivity (Fig. 6A,B). In contrast, the Pf comprised a large population of small neuronal perikarya that lay within a lightly stained neuropil (Fig. 6C). This pattern was the same across the whole rostrocaudal extent of the CM/Pf.

Ultrastructural Features of Lrrk2 Immunostaining in the Striatum

Because the striatum harbored a strong Lrrk2 neuropil immunoreactivity that could not be completely characterized at the light microscopic level, we used electron microscopy to further determine the cellular compartments that contained this immunoreactivity. Blocks of tissue from the pre- and post-commissural levels of the caudate nucleus and putamen were cut in ultrathin sections and examined under the electron microscope. To make sure that Lrrk2 antibodies had full access to antigenic sites, the quantitative data were collected exclusively from the most superficial sections of striatal tissue blocks.

Electron micrographs of immunoreactive elements from the striatum are shown in figure 6, while quantitative analyses of the relative percentages of labeled structures in the pre- and post-commissural striatum are depicted in figure 8. Overall, the pattern of Lrrk2 immunostaining was very similar between the caudate nucleus and putamen, without any significant rostrocaudal difference in the relative abundance of specific immunoreactive structures (Fig. 8). The majority of striatal Lrrk2 labeling was found in dendrites (40–60% of total immunoreactive elements), though terminals (10–30%) and unmyelinated axons (10–30%) also accounted for a significant proportion of labeled structures throughout the striatum, while glial processes were rarely seen (2–7%). There was no significant difference in the mean percentages of Lrrk2-immunoreactive neuronal elements between the pre-commissural caudate nucleus and putamen, while the post-commissural putamen contained a significantly lower percentage of Lrrk2-positive dendrites with a higher percentage of Lrrk2-immunostained terminals and glia than in the post-commissural caudate nucleus (t-test, $P<0.05$).

To further characterize the potential sources and transmitter phenotype of immunoreactive terminals, the labeled boutons were divided into three groups based on their synaptic specializations: (1) terminals that formed asymmetric synapses, (2) terminals that formed symmetric synapses and (3) terminals that did not display any distinctive synaptic junction in the plane of section examined. Of the 106 Lrrk2-immunoreactive terminals examined, 60% formed asymmetric synapses, 5% established symmetric synaptic contacts, while the remaining 35% did not display clear synaptic specializations.

In order to determine the relative abundance of immunoreactive dendrites and terminals forming asymmetric synapses over the total population of striatal elements in these

categories, we scanned series of micrographs of immunoreactive elements from the most superficial sections of the blocks and counted the total number of labeled and unlabeled dendritic shafts and asymmetric terminal profiles (Fig. 9). The mean (± S.E.M) percentage of labeled dendrites and terminals forming asymmetric synapses in the striatum was then calculated and compared statistically between the caudate nucleus and putamen. In both pre- and post-commissural striatum, the mean percentages of labeled dendrites were higher in the caudate nucleus (35.55% ± 4.40; 46.16% ± 1.48; pre- and post- striatum, respectively) than in the putamen (22.23% ± 2.98; 34.64% ± 1.32), whereas the opposite was found for the labeled asymmetric terminal profiles, which were more abundant in the putamen (14.37% ± 0.58; 18.93% ± 1.37) than the caudate nucleus (10.46% ± 1.31; 10.42% ± 0.68). The differences between the caudate nucleus and putamen were only significant in the post-commissural striatum (t-test, $P<0.05$).

Discussion

The results of this study provide the first detailed description of Lrrk2 protein distribution in the nonhuman primate basal ganglia. Overall, various features of Lrrk2 immunostaining pattern described in this study are congruent with results of previous studies in rodent and human brains, though some noticeable features are worth consideration. First, although the striatum was found to be the most enriched basal ganglia nuclei in Lrrk2 immunoreactivity in the monkey brain, as previously shown in other species, our findings provide additional evidence that the bulk of Lrrk2 labeling is confined to dendritic processes and axon terminals. These observations are consistent with recent *in vitro* data indicating that Lrrk2 interacts with cytoskeletal intracellular organelles and/or the microtubule network to regulate protein biogenesis and trafficking (Biskup et al., 2006; Greggio et al., 2006; Gandhi et al., 2008; Shin et al., 2008). In addition, the significant expression of Lrrk2 immunoreactivity in putative glutamatergic boutons is indicative of a potential role in the regulation of excitatory synaptic transmission at corticostriatal or thalamostriatal synapses. Although both the caudate nucleus and the putamen contained Lrrk2-immunoreactive dendrites and terminals, significant differences were found in the prevalence of labeled elements between the two major striatal components; the proportion of Lrrk2-labeled dendrites being higher in the caudate nucleus than the putamen, while the reverse was true for labeled axon terminals. Second, our data demonstrate a differential level of Lrrk2 immunoreactivity between GPe and GPi neurons in rhesus monkeys. Although the functional significance of this heterogeneous pattern of labeling between the two pallidal segments is unknown, these observations provide one of the rare evidence for differential chemical phenotypes between neuronal populations in the two pallidal segments in primates. Third, our data extend recent immunocytochemical findings supporting a strong expression of Lrrk2 in midbrain dopaminergic neurons, thereby suggesting that Lrrk2 mutations may directly interfere with the functioning of nigrostriatal dopaminergic neurons in Parkinson's disease. Finally, the centromedian nucleus, considered as the main source of thalamic projections to the sensorimotor striatum in primates (Smith et al., 2004, 2009), is devoid of Lrrk2 immunoreactivity, a feature strikingly different from the other thalamic nuclei, which are strongly enriched in Lrrk2 protein.

Together, these findings provide evidence for a widespread, but specific, expression of the Lrrk2 protein in the primate basal ganglia. Combined with a deeper characterization of Lrrk2 function, these data will contribute to a better understanding of the mechanisms by which Lrrk2 regulates normal basal ganglia function and participates in midbrain dopaminergic neurons degeneration in parkinsonian condition.

Lrrk2 protein expression in the basal ganglia and thalamus

In accordance with previous rodent and human studies (Melrose et al., 2007; Higashi et al., 2007a,b), the striatum was, by far, the most enriched brain region in Lrrk2 immunoreactivity in monkeys. Overall, the cellular and neuropil Lrrk2 labeling described in the monkey striatum is consistent with that observed in rodents and humans (Biskup et al., 2006; Higashi et al., 2007a,b; Melrose et al., 2007), i.e. light labeling of numerous small cell bodies of projection neurons and stronger immunoreactivity in large interneurons perikarya (Biskup et al., 2006; Higashi et al., 2007a,b; Melrose et al., 2007). Our co-localization data indicate that a significant subset of the Lrrk2-containing interneurons in monkeys are the parvalbumin-containing GABAergic fast spiking interneurons, known as the main sources of feedforward inhibition in the rat striatum (Tepper and Bolam, 2004; Mallet et al., 2005). In contrast, calretinin-containing interneurons, which represent the largest population of striatal interneurons in primates (Wu and Parent, 2000), were almost completely devoid of Lrrk2 labeling in monkeys. There are inconsistencies in the literature regarding the chemical phenotype of striatal interneurons enriched in Lrrk2 protein. On one hand, some reports indicate that Lrrk2 and parvalbumin, but not calretinin, frequently co-localize in mouse and human striatal interneurons (Biskup et al., 2006; Higashi et al., 2007a,b), while the same authors described in another study an almost complete overlap between calretinin and Lrrk2, with very limited parvalbumin/Lrrk2 co-localization in humans (Higashi et al., 2007b). The specificity of Lrrk2 antibodies, the possible down regulation of calcium binding proteins expression in postmortem striatal tissue and the sensitivity of the co-localization immunofluorescence methods on perfusion-fixed versus immersion-fixed striatal tissue may explain these conflicting data. Although not directly tested in our study, we expect that most cholinergic interneurons also express Lrrk2 immunoreactivity in monkeys. In contrast to the controversial data about the Lrrk2/calcium binding proteins co-existence, rodent and human studies, indeed, agree that almost all striatal cholinergic interneurons display Lrrk2 immunoreactivity (Biskup et al., 2006; Higashi et al., 2007a,b).

Albeit not as strong as in the striatum, other basal ganglia nuclei including the GPe, the STN and the SNc/VTA also display light to moderate Lrrk2 immunoreactivity in monkeys. In contrast to the consistent report of Lrrk2 protein expression in midbrain dopaminergic neurons of primates and nonprimates (Biskup et al., 2006; Higashi et al., 2007b; Melrose et al., 2007), there has been significant inconsistencies across studies regarding the level of *LRRK2* mRNA expression in these neurons (Galter et al., 2006; Melrose et al., 2006, Simon-Sanchez et al., 2006; Taymans et al., 2006; Higashi et al., 2007b). Whether this discrepancy between Lrrk2 protein and mRNA localization in nigral neurons is the result of differences in sensitivity between the protein and mRNA detection methods, or a genuine difference in the translation of *LRRK2* mRNA into protein remains to be determined (Gandhi et al., 2009). Data obtained so far are unclear about the possible role of Lrrk2 in dopamine neurotransmission. Current evidence suggests that changes in dopamine release and severe striatal dopamine depletion have little, if any, effects of striatal Lrrk2 protein and mRNA expression (Galter et al., 2006; Higashi et al., 2007b; Gandhi et al., 2009).

An interesting, though surprising, finding of this study was the differential expression level of Lrrk2 protein expression between GPe and GPi neurons and the strong immunoreactivity associated with putative cholinergic neurons in the nucleus basalis of Meynert (NBM), two features that have not been reported in previous rat and human studies (Higashi et al., 2007a,b; Melrose et al., 2007). To our knowledge, very few markers are differentially expressed between GPe and GPi neurons, one exception being the AMPA GluR1 subunit which was found to be significantly more abundant in GPe than GPi neurons in squirrel monkeys (Paquet and Smith, 1996). The NBM cholinergic neurons are also enriched in GluR1, thereby providing a pattern of GluR1 labeling in the pallidal complex and basal forebrain that strikingly mimics that described for Lrrk2 in the present study. Because of the

limited knowledge of Lrrk2 function and its possible interacting proteins in the CNS, the significance of this correlation in labeling pattern between Lrrk2 and AMPA GluR1 subunit is unknown.

Our findings indicate that most thalamic nuclei in monkey are enriched in Lrrk2 immunoreactivity, a finding consistent with some rodent immunohistochemical data (Melrose et al., 2007), but at odds with *in situ* hybridization studies that showed low to moderate levels of *LRRK2* mRNA expression in the mouse thalamus, except in the reticular nucleus (Melrose et al., 2006; Simon-Sanchez et al., 2006; Higashi et al., 2007a). Although the *LRRK2* mRNA localization has not been achieved in the monkey brain, the apparent discrepancy between the level of Lrrk2 protein expression described in our study and previous rodent mRNA data suggest that, like the SNc, the thalamus is another brain region where the correlation between *LRRK2* gene and protein expression must be interpreted with great caution. In contrast to most thalamic nuclei, the centromedian nucleus was almost completely devoid of Lrrk2 immunoreactivity in monkeys. The significance of this differential expression level of Lrrk2 protein between the CM and the rest of the thalamus is unclear, but it is worth noting that other proteins, like calbindin D28K and calretinin which are widely expressed in most thalamic neurons are also completely absent from CM neurons (Jones and Hendry, 1989; Fortin et al., 1996; Percheron et al., 1996). Another important feature that characterizes CM neurons over other thalamic nuclei is their significant degeneration in patients with Parkinson's disease (Henderson et al., 2000a,b; Halliday et al., 2005). Future studies are needed to fully understand the functional significance of these observations and elucidate the role Lrrk2 may play in regulating neuronal activity in the thalamus.

Ultrastructural localization of Lrrk2 in the striatum

Our data indicate that Lrrk2 is strongly expressed in dendritic shafts and subsets of putative glutamatergic terminals in the monkey striatum. Overall, these observations are consistent with qualitative data previously obtained in rodent brains and culture cells showing that Lrrk2 immunoreactivity is associated with vesicular and membranous structures, the microtubule network, synaptic vesicles and other membrane-bound organelles (West et al., 2005; Biskup et al., 2006; Gloeckner et al., 2006; Greggio et al., 2006; Hatano et al. 2007; Kingsbury et al., 2008; Gandhi et al., 2008, 2009). Although the level of resolution offered by the immunoperoxidase method used in our study limits considerably the analysis of Lrrk2 expression at the subcellular level, the strong association with membranous structures and synaptic vesicles is unequivocal, which is consistent with the proposed hypothesis that Lrrk2 may play a role in the biogenesis or regulation of vesicular structures, vesicular transport, neuronal growth and possibly protein turnover (Biskup et al., 2006; MacLeod et al., 2006; Gandhi et al., 2009; Gillardon, 2009; Parisiadou et al., 2009). Although the sources of immunolabeled terminals have not been characterized in our study, the fact that they all form axo-spinous asymmetric synapses indicates that they originate from the cerebral cortex or the thalamus (Smith et al., 2004, 2009; Raju et al., 2006; Smith and Villalba, 2008). Knowing that abnormal glutamatergic transmission at corticostriatal synapses is a key pathophysiological feature of Parkinson's disease (Calabresi et al., 2007), our findings suggest that Lrrk2 mutation may contribute to the dysfunction of corticostriatal communication in parkinsonism.

Concluding Remarks

Since the first evidence that mutations of *LRRK2* gene is the most common cause of familial Parkinson's disease (Funayama et al., 2002), the characterization of the localization, function and molecular features of *LRRK2* has been at the forefront of research in various laboratories. Despite the large amount of data that have resulted from these studies, the exact

functional characteristics of *LRRK2* in the brain remain poorly understood. The recent evidence for interactions with proteins involved in regulating neurite outgrowth and morphology suggest that Lrrk2 may play an important role in neuronal development and morphological plasticity associated with normal and abnormal brain functions (MacLeod et al., 2006; Jaleel et al., 2007; Gandhi et al., 2009; Parisiadou et al., 2009). However, the lack of information on Lrrk2-interacting proteins and the related signaling cascades limits considerably our understanding of the mechanisms underlying *LRRK2*-mediated effects in the CNS. Thus, a deeper knowledge of the pathological effects of *LRRK2* mutations in Parkinson's disease rely on further characterization of the physiological role and substrates of Lrrk2 in the normal CNS.

Acknowledgments

This work was supported by the NIH base grant of the Yerkes National Primate Research Centre (RR-00165), the Parkinson's Disease Foundation (fellowship award to HM) and the Morris Udall Parkinson's Disease Centre of Excellence (P50 NS40256). Thanks are due to Susan Jenkins for technical assistance.

REFERENCES

Anand VS, Braithwaite SP. LRRK2 in Parkinson's disease: biochemical functions. FEBS J. 2009 (in press).

Biskup S, Moore DJ, Celsi F, Higashi S, West AB, Andrabi SA, Kurkinen K, Yu SW, Savitt JM, Waldvogel HJ, Faull RL, Emson PC, Torp R, Ottersen OP, Dawson TM, Dawson VL. Localization of LRRK2 to membranous and vesicular structures in mammalian brain. Ann. Neurol 2006;60:557–569.

Calabresi P, Picconi B, Tozzi A, Di Filippo M. Dopamine-mediated regulation of corticostriatal synaptic plasticity. Trends Neurosci 2007;30:211–219. [PubMed: 17367873]

Celio MR, Baier W, Scharer L, de Viragh PA, Gerday C. Monoclonal antibodies directed against the calcium binding protein parvalbumin. Cell Calcium 1988;9:81–86. [PubMed: 3383226]

Covy JP, Yuan W, Waxman EA, Hurtig HI, Van Deerlin VM, Giasson BI. Clinical and pathological characteristics of patients with leucine-rich repeat kinase-2 mutations. Mov. Disord 2009;24:32–39.

Fortin M, Asselin MC, Parent A. Calretinin immunoreactivity in the thalamus of the squirrel monkey. J. Chem. Neuroanat 1996;10:101–117. [PubMed: 8783040]

Funayama M, Hasegawa K, Kowa H, Saito M, Tsuji S, Obata F. A new locus for Parkinson's disease (PARK8) maps to chromosome 12p11.2-q13.1. Ann. Neurol 2002;51:296–301. [PubMed: 11891824]

Galter D, Westerlund M, Carmine A, Lindqvist E, Sydow O, Olson L. LRRK2 expression linked to dopamine-innervated areas. Ann Neurol 2006;59:714–719. [PubMed: 16532471]

Gandhi PN, Wang X, Zhu X, Chen SG, Wilson-Delfosse AL. The Roc domain of leucine-rich repeat kinase 2 is sufficient for interaction with microtubules. J Neurosci Res 2008;86:1711–1720. [PubMed: 18214993]

Gandhi PN, Chen SG, Wilson-Delfosse AL. Leucine-rich repeat kinase 2 (LRRK2): a key player in the pathogenesis of Parkinson's disease. J Neurosci Res 2009;87:1283–1295. [PubMed: 19025767]

Gasser T. Molecular pathogenesis of Parkinson's disease: insights from genetic studies. Expert Rev Mol Med 2009;11:e22. [PubMed: 19631006]

Giasson BI, Covy JP, Bonini NM, Hurtig HI, Farrer MJ, Trojanowski JQ, Van Deerlin VM. Biochemical and pathological characterization of Lrrk2. Ann Neurol 2006;59:315–322. [PubMed: 16437584]

Gillardon F. Leucine-rich repeat kinase 2 phosphorylates brain tubulin-beta isiforms and modulates microtubule stability—a point of convergence in parkinsonian neurodegeneration? J Neurochem 2009;110:1514–1522. [PubMed: 19545277]

Gloeckner CJ, Kinkl N, Schumacher A, Braun RJ, O'Neill E, Meitinger T, Kolch W, Prokisch H, Ueffing M. The Parkinson disease causing LRRK2 mutation I2020T is associated with increased kinase activity. Hum Mol Genet 2006;15:223–232. [PubMed: 16321986]

Greggio E, Jain S, Kingsbury A, Bandopadhyay R, Lewis P, Kaganovich A, van der Brug MP, Beilina A, Blackinton J, Thomas KJ, Ahmad R, Miller DW, Kesavapany S, Singleton A, Lees A, Harvey RJ, Harvey K, Cookson MR. Kinase activity is required for the toxic effects of mutant LRRK2/dardarin. Neurobiol Dis 2006;23:329–341. [PubMed: 16750377]

Halliday GM, Macdonald V, Henderson JM. A comparison of degeneration in motor thalamus and cortex between progressive supranuclear palsy and Parkinson's disease. Brain 2005;128:2272–2280. [PubMed: 16014651]

Hatano T, Kubo S, Imai S, Maeda M, Ishikawa K, Mizuno Y, Hattori N. Leucine-rich repeat kinase 2 associates with lipid rafts. Hum Mol Genet 2007;16:678–690. [PubMed: 17341485]

Henderson JM, Carpenter K, Cartwright H, Halliday GM. Loss of thalamic intralaminar nuclei in progressive supranuclear palsy and Parkinson's disease: clinical and therapeutic implications. Brain 2000a;123(Pt 7):1410–1421. [PubMed: 10869053]

Henderson JM, Carpenter K, Cartwright H, Halliday GM. Degeneration of the centre median-parafascicular complex in Parkinson's disease. Ann Neurol 2000b;47:345–352. [PubMed: 10716254]

Higashi S, Biskup S, West AB, Trinkaus D, Dawson VL, Faull RL, Waldvogel HJ, Arai H, Dawson TM, Moore DJ, Emson PC. Localization of Parkinson's disease-associated LRRK2 in normal and pathological human brain. Brain Res 2007a;1155:208–219. [PubMed: 17512502]

Higashi S, Moore DJ, Colebrooke RE, Biskup S, Dawson VL, Arai H, Dawson TM, Emson PC. Expression and localization of Parkinson's disease-associated leucine-rich repeat kinase 2 in the mouse brain. J Neurochem 2007b;100:368–381. [PubMed: 17101029]

Higashi S, Moore DJ, Yamamoto R, Minegishi M, Sato K, Togo T, Katsuse O, Uchikado H, Furukawa Y, Hino H, Kosaka K, Emson PC, Wada K, Dawson VL, Dawson TM, Arai H, Iseki E. Abnormal localization of leucine-rich repeat kinase 2 to the endosomal-lysosomal compartment in Lewy body disease. J Neuropathol Exp Neurol 2009;68:994–1005. [PubMed: 19680143]

Jaleel M, Nichols RJ, Deak M, Campbell DG, Gillardon F, Knebel A, Alessi DR. LRRK2 phosphorylates moesin at threonine-558: characterization of how Parkinson's disease mutants affect kinase activity. Biochem J 2007;405:307–317. [PubMed: 17447891]

Jones EG, Hendry SH. Differential Calcium Binding Protein Immunoreactivity Distinguishes Classes of Relay Neurons in Monkey Thalamic Nuclei. Eur J Neurosci 1989;1:222–246. [PubMed: 12106154]

Lesage S, Leutenegger AL, Brice A. [LRRK2: a gene belonging to the ROCO family is implicated in the Parkinson's disease]. Med Sci (Paris) 2005;21:1015–1017. [PubMed: 16324633]

Lesage S, Durr A, Brice A. LRRK2: a link between familial and sporadic Parkinson's disease? Pathol Biol (Paris) 2007;55:107–110. [PubMed: 16884863]

Liou GY, Gallo KA. New biochemical approaches towards understanding the Parkinson’s disease-associated kinase, LRRK2. Biochem J 2009;424:e1–e3. [PubMed: 19839940]

MacLeod D, Dowman J, Hammond R, Leete T, Inoue K, Abeliovich A. The familial Parkinsonism gene LRRK2 regulates neurite process morphology. Neuron 2006;52:587–593. [PubMed: 17114044]

Mallet N, Le Moine C, Charpier S, Gonon F. Feedforward inhibition of projection neurons by fast-spiking GABA interneurons in the rat striatum in vivo. J Neurosci 2005;25:3857–3869. [PubMed: 15829638]

Mata IF, Wedemeyer WJ, Farrer MJ, Taylor JP, Gallo KA. LRRK2 in Parkinson's disease: protein domains and functional insights. Trends Neurosci 2006;29:286–293. [PubMed: 16616379]

Melrose H, Lincoln S, Tyndall G, Dickson D, Farrer M. Anatomical localization of leucine-rich repeat kinase 2 in mouse brain. Neuroscience 2006;139:791–794. [PubMed: 16504409]

Melrose HL, Kent CB, Taylor JP, Dachsel JC, Hinkle KM, Lincoln SJ, Mok SS, Culvenor JG, Masters CL, Tyndall GM, Bass DI, Ahmed Z, Andorfer CA, Ross OA, Wszolek ZK, Delldonne A, Dickson DW, Farrer MJ. A comparative analysis of leucine-rich repeat kinase 2 (Lrrk2) expression in mouse brain and Lewy body disease. Neuroscience 2007;147:1047–1058. [PubMed: 17611037]

Melrose H. Update on the functional biology of Lrrk2. Future Neurol 2008;3:669–681. [PubMed: 19225574]

Miklossy J, Arai T, Guo JP, Klegeris A, Yu S, McGeer EG, McGeer PL. LRRK2 expression in normal and pathologic human brain and in human cell lines. J Neuropathol Exp Neurol 2006;65:953–963. [PubMed: 17021400]

Paquet M, Smith Y. Differential localization of AMPA glutamate receptor subunits in the two segments of the globus pallidus and the substantia nigra pars reticulata in the squirrel monkey. Eur J Neurosci 1996;8:229–233. [PubMed: 8713467]

Parisiadou L, Xie C, Cho HJ, Lin X, Gu XL, Long CX, Lobbestael E, Baekelandt V, Taymans JM, Sun L, Cai H. Phosphorylation of ezrin/radixin/moesin proteins by LRRK2 promotes the rearrangement of actin cytoskeleton in neuronal morphogenesis. J Neurosci 2009;29:13971–13980. [PubMed: 19890007]

Percheron G, Francois C, Talbi B, Yelnik J, Fenelon G. The primate motor thalamus. Brain Res Brain Res Rev 1996;22:93–181. [PubMed: 8883918]

Qing H, Zhang Y, Deng Y, McGeer EG, McGeer PL. Lrrk2 interaction with alpha-synuclein in diffuse Lewy body disease. Biochem Biophys Res Commun 2009;390:1229–1234. [PubMed: 19878656]

Raju DV, Shah DJ, Wright TM, Hall RA, Smith Y. Differential synaptology of vGluT2-containing thalamostriatal afferents between the patch and matrix compartments in rats. J Comp Neurol 2006;499:231–243. [PubMed: 16977615]

Shin N, Jeong H, Kwon J, Heo HY, Kwon JJ, Yun HJ, Kim CH, Han BS, Tong Y, Shen J, Hatano T, Hattori N, Kim KS, Chang S, Seol W. LRRK2 regulates synaptic vesicle endocytosis. Exp Cell Res 2008;314:2055–2065. [PubMed: 18445495]

Simon-Sanchez J, Herranz-Perez V, Olucha-Bordonau F, Perez-Tur J. LRRK2 is expressed in areas affected by Parkinson's disease in the adult mouse brain. Eur J Neurosci 2006;23:659–666. [PubMed: 16487147]

Smith, Y.; Bolam, JP. Combined approaches to experimental neuroanatomy: combined tracing and imunocytochemical techniques for the study of neuronal microcircuits. In: Bolam, JP., editor. Practical approach series; "Experimental Neuroanatomy: A practical approach". Oxford, UK: Oxford University Press; 1992. p. 239-266.

Smith Y, Raju DV, Pare JF, Sidibe M. The thalamostriatal system: a highly specific network of the basal ganglia circuitry. Trends Neurosci 2004;27:520–527. [PubMed: 15331233]

Smith WW, Pei Z, Jiang H, Dawson VL, Dawson TM, Ross CA. Kinase activity of mutant LRRK2 mediates neuronal toxicity. Nat Neurosci 2006;9:1231–1233. [PubMed: 16980962]

Smith Y, Villalba R. Striatal and extrastriatal dopamine in the basal ganglia: an overview of its anatomical organization in normal and Parkinsonian brains. Mov Disord 23 Suppl 2008;3:S534–S547.

Smith Y, Raju D, Nanda B, Pare JF, Galvan A, Wichmann T. The thalamostriatal systems: anatomical and functional organization in normal and parkinsonian states. Brain Res Bull 2009;78:60–68. [PubMed: 18805468]

Taylor JP, Mata IF, Farrer MJ. LRRK2: a common pathway for parkinsonism, pathogenesis and prevention? Trends Mol Med 2006;12:76–82. [PubMed: 16406842]

Taymans JM, Van den Haute C, Baekelandt V. Distribution of PINK1 and LRRK2 in rat and mouse brain. J Neurochem 2006;98:951–961. [PubMed: 16771836]

Tepper JM, Bolam JP. Functional diversity and specificity of neostriatal interneurons. Curr Opin Neurobiol 2004;14:685–692. [PubMed: 15582369]

Villalba RM, Lee H, Smith Y. Dopaminergic denervation and spine loss in the striatum of MPTP-treated monkeys. Exp Neurol 2009;215:220–227. [PubMed: 18977221]

Waxman EA, Covy JP, Bukh I, Li X, Dawson TM, Giasson BI. Leucone-rich repeat kinase 2 expression leads to aggresome formation that is not associated with alpha-synuclein inclusions. J Neuropathol Exp Neurol 2009;68:785–796. [PubMed: 19535993]

West AB, Moore DJ, Choi C, Andrabi SA, Li X, Dikeman D, Biskup S, Zhang Z, Lim KL, Dawson VL, Dawson TM. Parkinson's disease-associated mutations in LRRK2 link enhanced GTP-binding and kinase activities to neuronal toxicity. Hum Mol Genet 2007;16:223–232. [PubMed: 17200152]

Westerlund M, Belin AC, Anvret A, Bickford P, Olson L, Galter D. Developmental regulation of leucine-rich repeat kinase 1 and 2 expression in the brain and other rodent and human organs: Implications for Parkinson's disease. Neuroscience 2008;152:429–436. [PubMed: 18272292]

Wu Y, Parent A. Striatal interneurons expressing calretinin, parvalbumin or NADPH-diaphorase: a comparative study in the rat, monkey and human. Brain Res 2000;863:182–191. [PubMed: 10773206]

Zhu X, Babar A, Siedlak SL, Yang Q, Ito G, Iwatsubo T, Smith MA, Perry G, Chen SG. LRRK2 in Parkinson's disease and dementia with Lewy bodies. Mol Neurodegener 2006a;1:17. [PubMed: 17137507]

Zhu X, Siedlak SL, Smith MA, Perry G, Chen SG. LRRK2 protein is a component of Lewy bodies. Ann Neurol 2006b;60:617–618. author reply 618–619. [PubMed: 16847950]

Zimmermann L, Schwaller B. Monoclonal antibodies recognizing epitopes of calretinin. Dependence of Ca2+-binding status and difference in antigen accessibility in colon cancer cells. Cell Calcium 2002;31:13–25. [PubMed: 11990296]

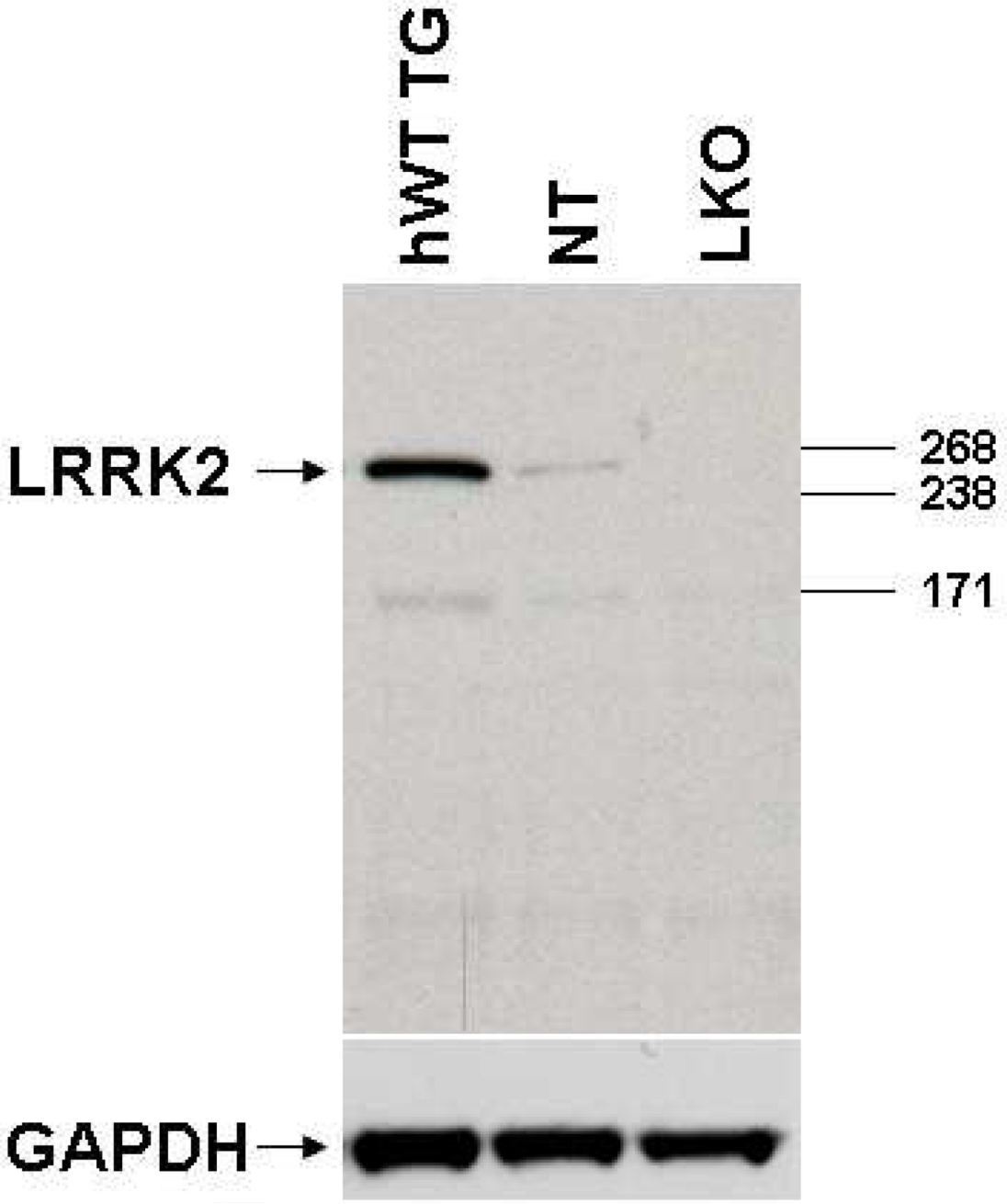

Figure 1.
Western immunoblot of the polyclonal LRRK2 antiserum PA0362 (Novus Biologicals-NB110-58771SS) showing that these Lrrk2 antibodies detect a single band that corresponds to the molecular weight (approximately 280kd) of Lrrk2 protein when run against hWT TG (BAC mice expressing human wild type Lrrk2) and murine Lrrk2 in NT (non-transgenic control), but do not detect any band labeling when applied on LKO (*LRRK2* Knockout mouse) brain tissue.

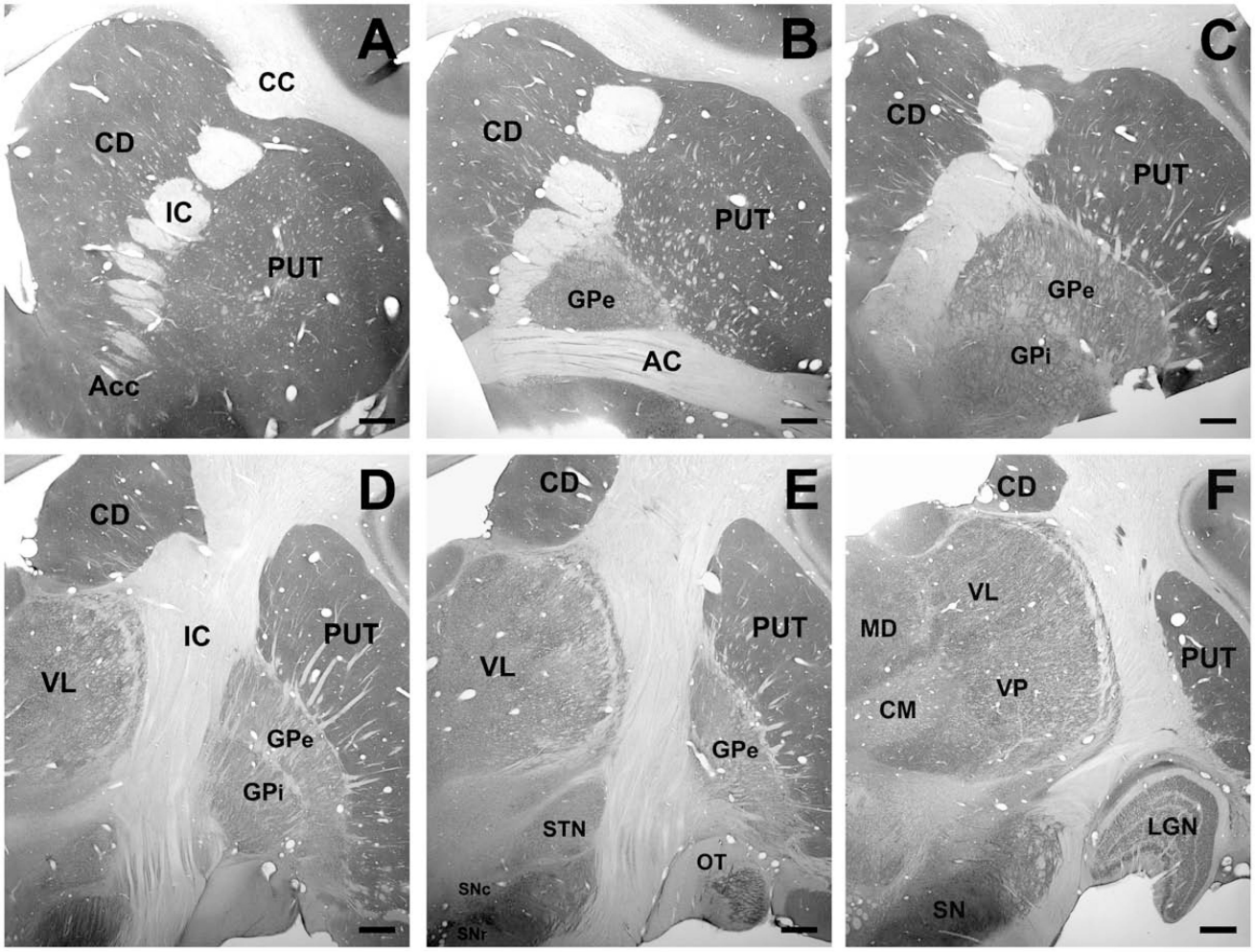

Figure 2.

(A–F) Lrrk2 immunoreactivity through the rostrocaudal extent of the monkey basal ganglia and thalamus. Scale bar in A–F: 1mm. Abbreviations: AC = anterior commissure; Acc = nucleus accumbens; CC = corpus callosum; CD = caudate nucleus; CM = centromedian thalamic nucleus; GPe = external segment of globus pallidus; GPi = internal segment of globus pallidus; IC = internal capsule; LGN = lateral geniculate nucleus; MD = mediodorsal nucleus; OT = olfactory tubercle; PUT = putamen; SNc = substantia nigra pars compacta; SNr = substantia nigra pars reticulata; STN = subthalamic nucleus; VL = ventrolateral nucleus; VP = ventroposterior nucleus; VTA = ventral tegmental area.

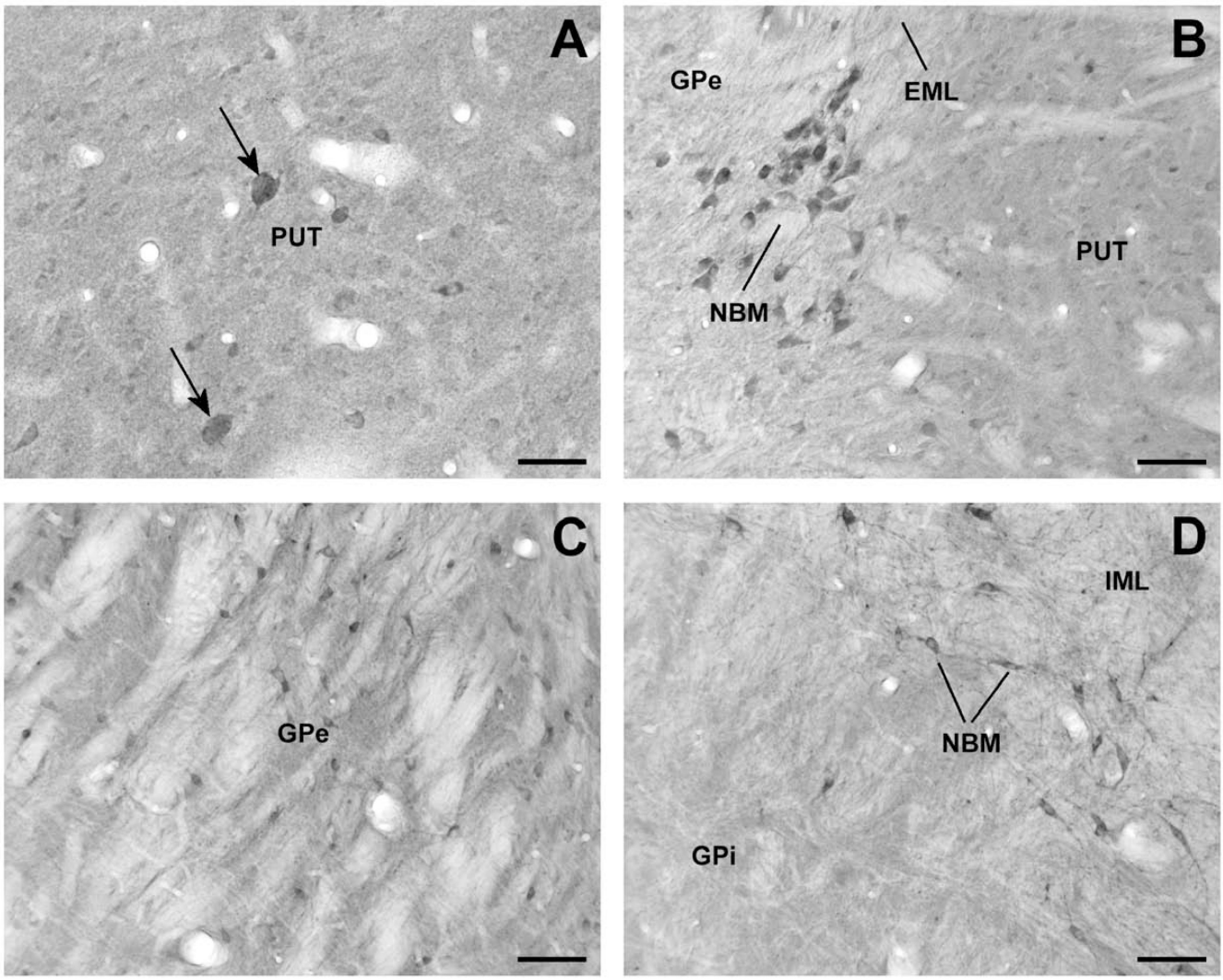

Figure 3.

Lrrk2-immunoreactive elements in the monkey striatopallidal complex and nucleus basalis of Meynert (NBM). (A) High-power micrograph of large cell bodies (arrow) and numerous small Lrrk2-immunoreactive perikarya in the putamen (PUT). (B) A cluster of Lrrk2-immunoreactive neurons that correspond to cholinergic NBM cells lying along the external medullary lamina (EML), between the PUT and GPe. (C) Lrrk2-immunoreactive neuronal profiles in GPe. (D) High magnification micrograph showing a lack of immunoreactive neurons in the internal segment of globus pallidus (GPi) in contrast to strong immunopositive neurons of NBM that lie along the internal medullary lamina (IML). Scale bars = 50 μm (A); 100 μm (B – D).

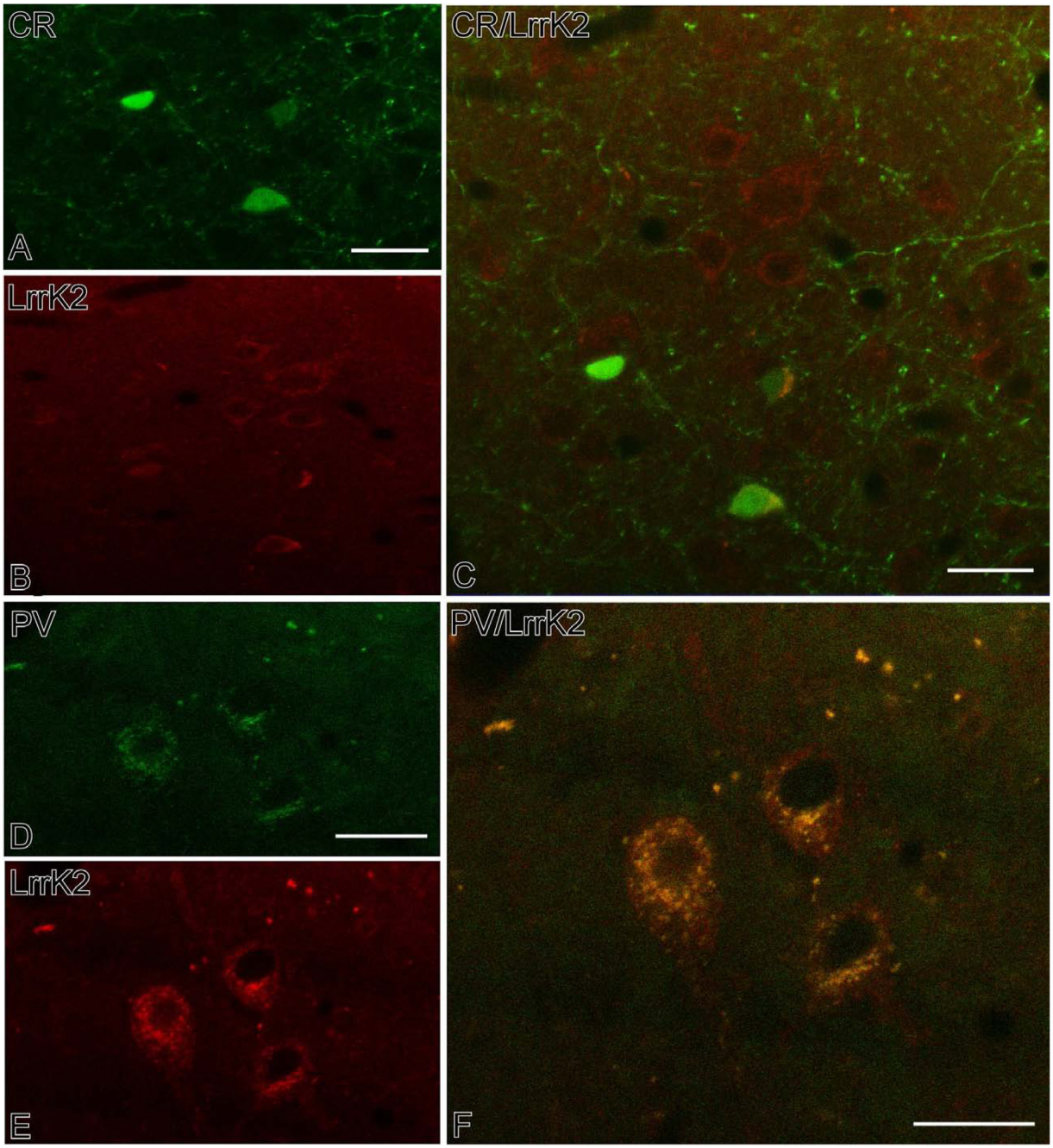

Figure 4.

Confocal double immunofluorescent micrographs showing results of co-localization experiments of CR (A–C) or PV (D–F) with Lrrk2 in subpopulations of striatal interneurons. In both sets of experiments, CR or PV imunoreactivity was labeled with FITC, while Lrrk2 immnostaining was revealed with TRITC. The panels in C and F show the overlap between the different markers. Notice the high degree of co-localization between PV and Lrrk2 (F) compared with the strict segregation of CR and Lrrk2 in different neuronal populations (C). Scale bars: A: 30 μm (valid for B); C: 30 μm; D: 20 μm (valid for E); F:20 μm.

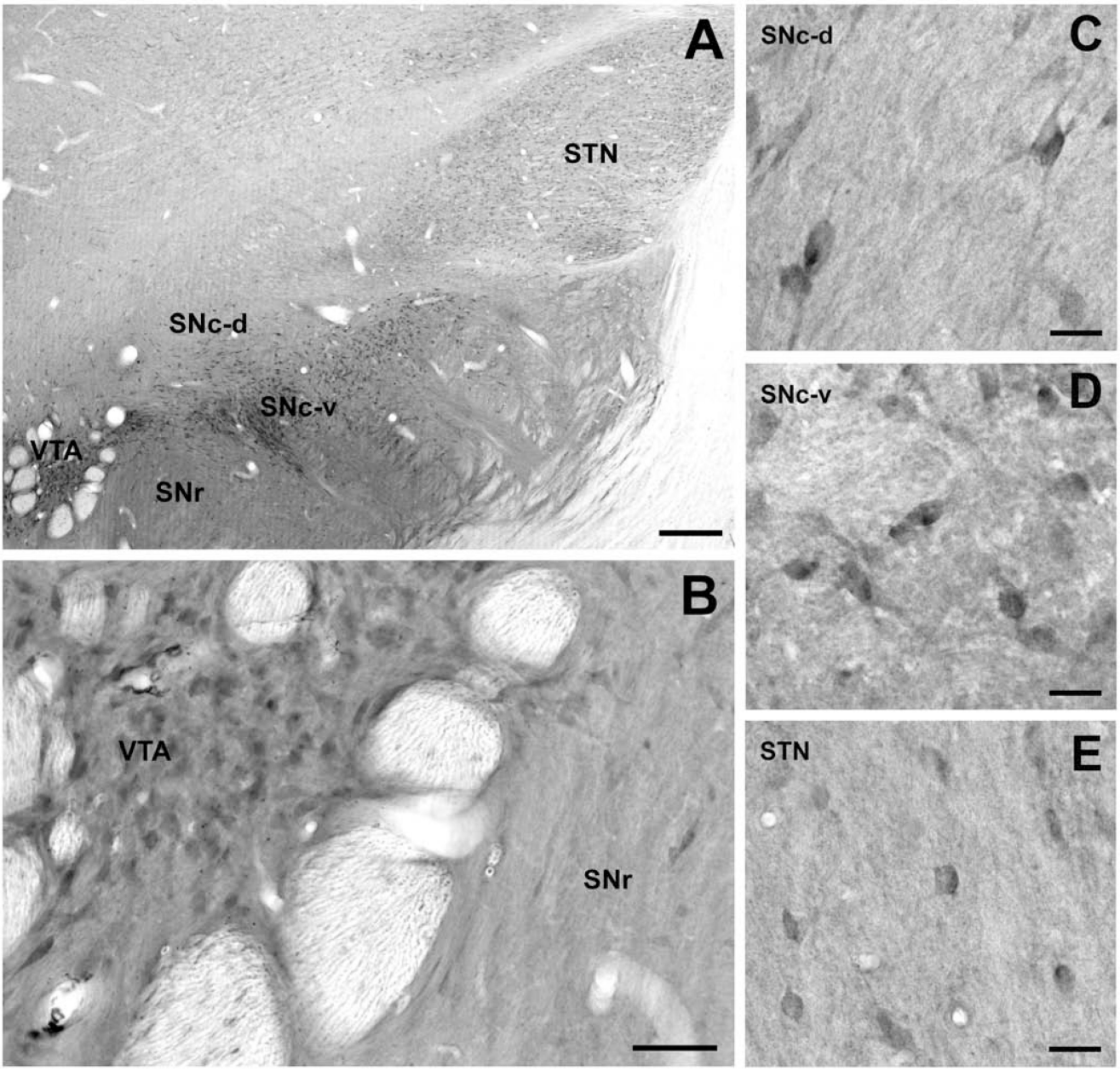

Figure 5.

Lrrk2 immunostaining in the subthalamic nucleus (STN) and ventral midbrain. (A) Low-power overview of Lrrk2 immunostaining in the STN, the dorsal and ventral tiers of SNc (SNc-d, SNc-v), the ventral tegmental area (VTA), and the substantia nigra pars reticulata (SNr). (B) A group of Lrrk2-immunoreactive, presumably dopaminergic, neurons that lay within a strongly labeled neuropil in the VTA and lightly labeled neurons of the SNr. (C, D) High-power micrographs of Lrrk2-immunoreactive neurons in the SNc-d and SNc-v. (E) Lrrk2-positive neuronal cell body profiles within a lightly labeled neuropil in the STN. Scale bars = 500 μm (A); 100 μm (B); 50 μm (C – E).

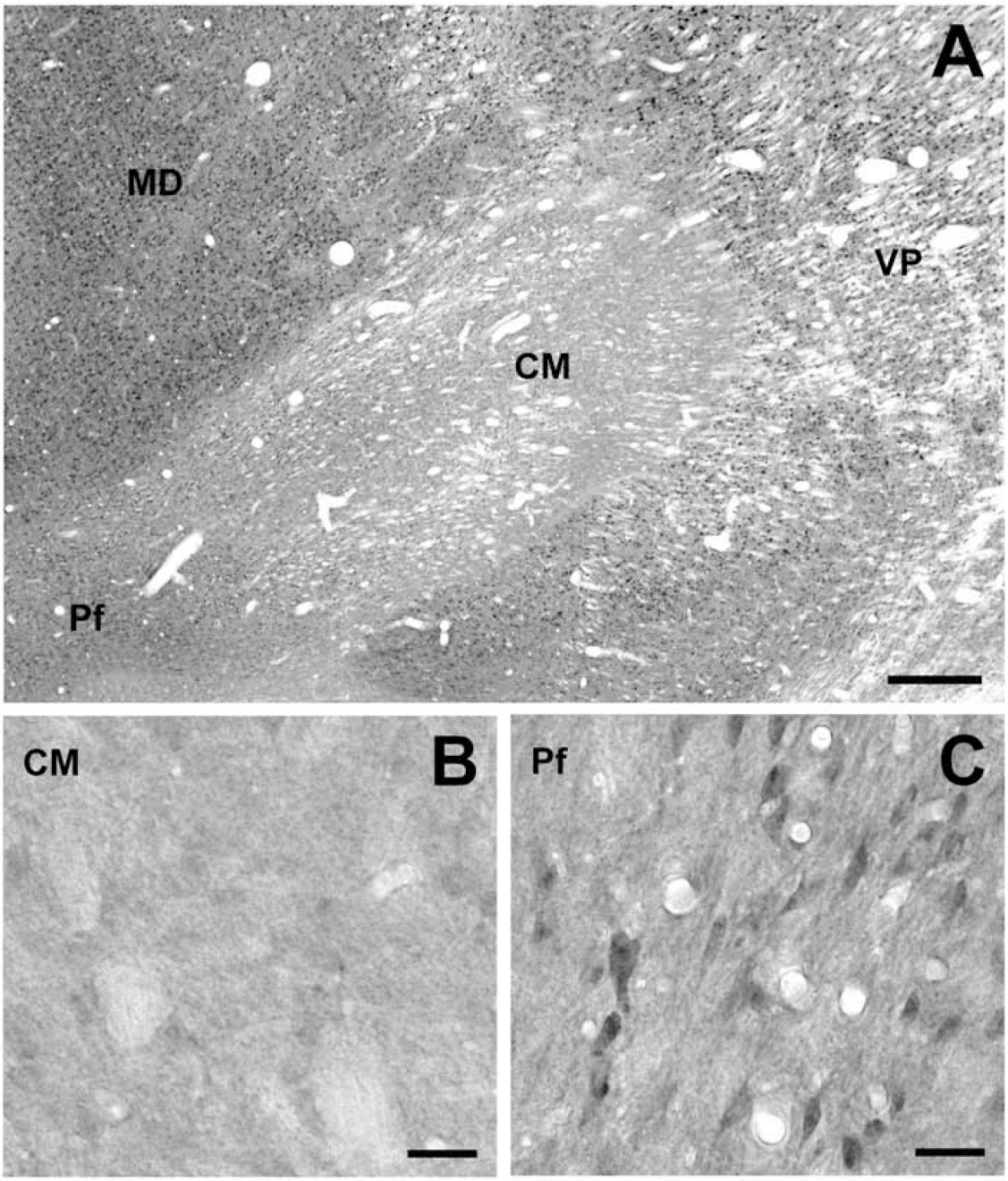

Figure 6.
Immunohistochemical localization of Lrrk2 in the monkey thalamus. (A) Low-power view of Lrrk2 immunoreactivity in the CM/Pf and surrounding thalamic nuclei including the mediodorsal (MD) and ventroposterior nuclei (VP). Note the striking contrast between the level of Lrrk2 immunoreactivity in CM copmpared to other thalamic nuclei. (B, C) Lack of significant Lrrk2 immunostaining in the CM compared with moderate to strong immunostaining in the Pf. Scale bars = 500 μm (A); 50 μm (B, C).

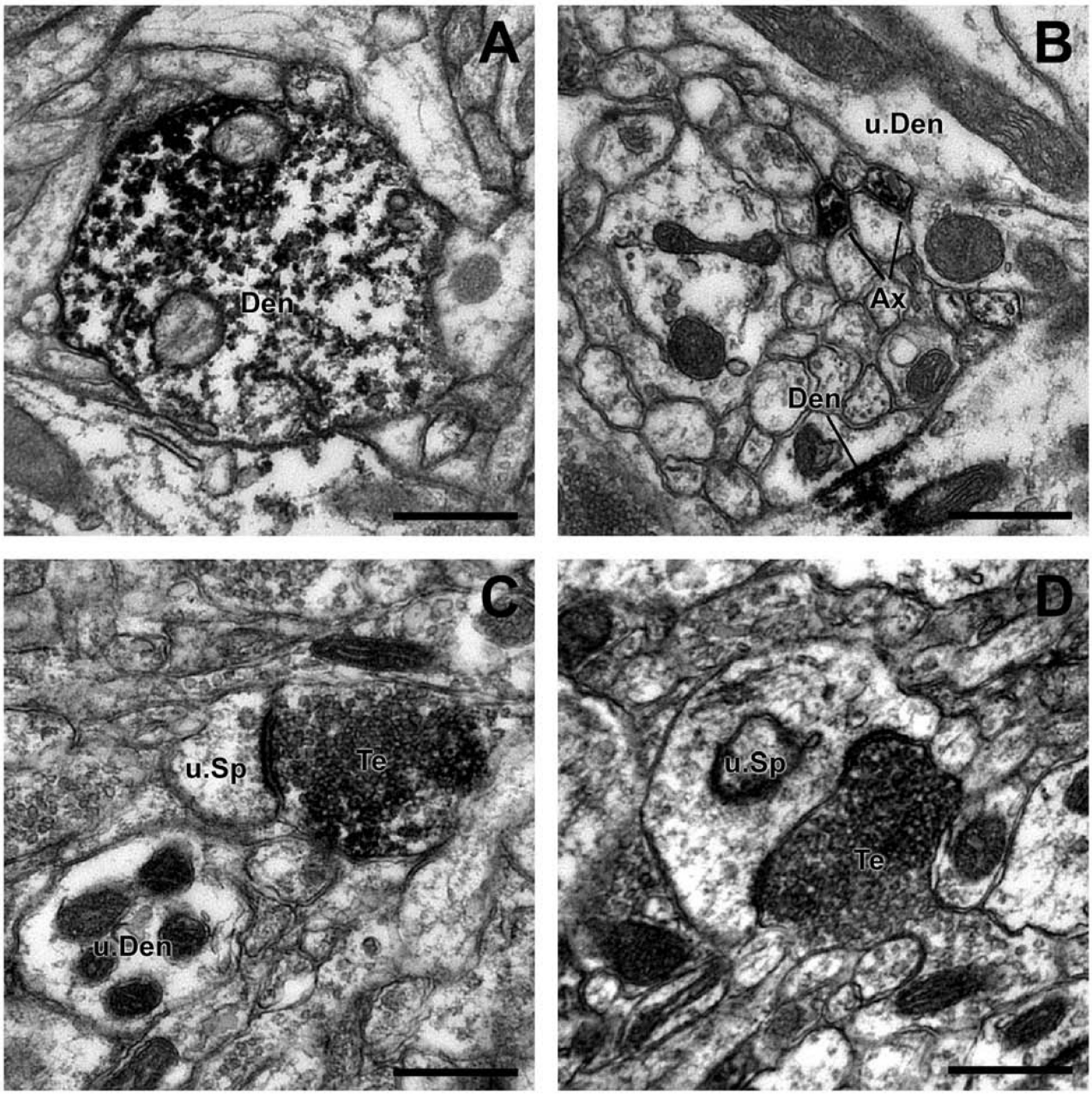

Figure 7.

Electron micrographs of Lrrk2-immunoreactive profiles in the monkey striatum. (A) A Lrrk2-positive dendritic shaft (Den) in the PUT. Note the dense peroxidase labeling attached to microtubules. (B) Lrrk2-immunoreactive unmyelinated axons (Ax) in the vicinity of an immunoreactive dendrite (Den) and an unlabeled dendrite (u.Den). (C,D) Two Lrrk2-positive terminals (Te) forming asymmetric synapses with unlabeled spines (u.sp). Scale bars = 0.5 μm.

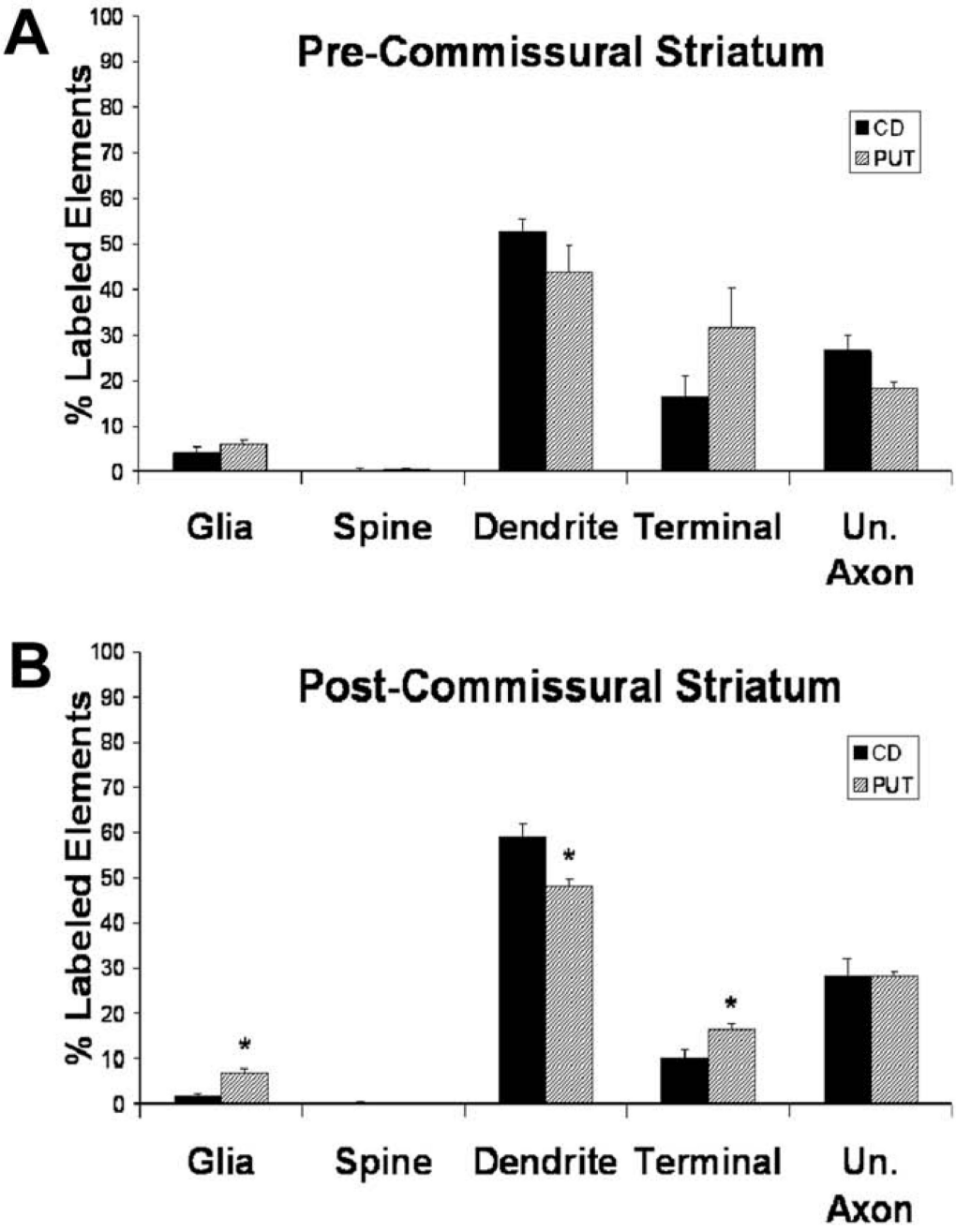

Figure 8.

Histograms comparing the mean (+/− SEM) percentages of the different categories of Lrrk2-immunopositive elements in the pre- (A) and post-commissural (B) caudate nucleus and putamen (n=3). Total number of labeled elements analyzed in the pre-commissural striatum: CD:518; PUT:383. Total number of immunopositive elements analyzed in the post-commissural striatum: CD: 615; PUT: 544. The average total surface of tissue examined per monkey is: pre-commissural striatum: CD: 1281.1μm^2; PUT: 1318.8μm^2; post-commissural striatum: CD: 1318.8μm^2; PUT: 1281.1μm^2. Abbreviations: CD: caudate nucleus; PUT: putamen; Un. Axon: unmyelinated axon. Asterisks indicate significant differences between CD and PUT ($P<0.05$; Student's t Test)

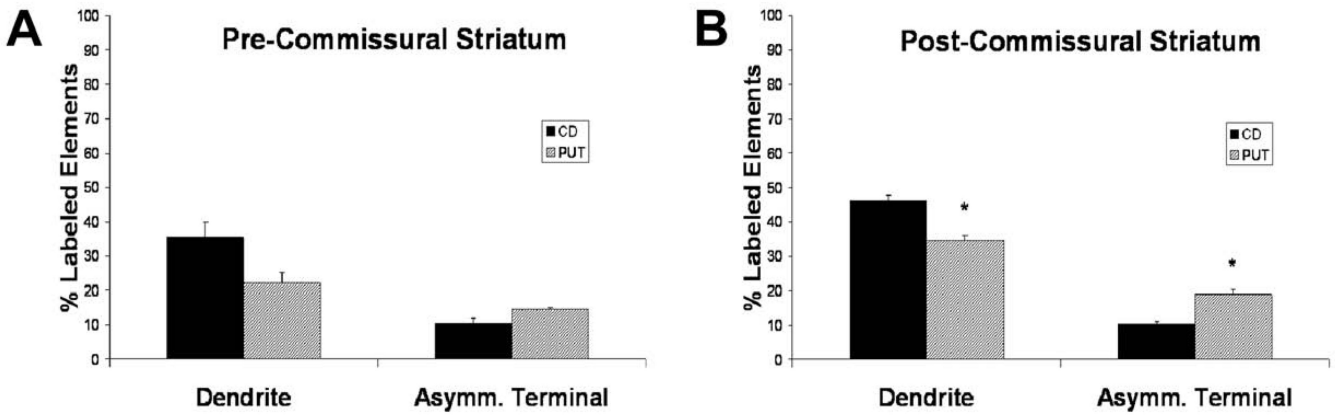

Figure 9.

The mean percentages (+/− SEM) of Lrrk2-immunolabeled dendrites and terminals forming asymmetric synapses in the pre- (A) and post- (B) commissural caudate nucleus and putamen (n=3). The total number of dendrites (labeled + unlabeled) examined in the pre-commissural striatum: CD: 782; PUT: 752, and in the post-commissural striatum: CD: 781; PUT: 780. The total number of terminals forming an asymmetric synapses (labeled, unlabeled, respectively) counted in the pre-commissural striatum: CD: 443; PUT: 508, and in the post-commissural striatum: CD: 397; PUT: 462. The average total surface of striatal tissue examined per monkey in the pre-commissural striatum: CD: 1281.1μm^2; PUT: 1318.8μm^2, and in the post-commissural striatum: CD: 1318.8μm^2; PUT: 1281.1μm^2. Abbreviations: CD: caudate nucleus; PUT: putamen; Asymm. Terminal: terminal forming an asymmetric synapse. Asterisks indicate significant differences between CD and PUT ($P<0.05$; Student's t Test)